ARTICLE

A. Tone · K. Shikata · M. Sasaki · S. Ohga · K. Yozai ·
S. Nishishita · H. Usui · R. Nagase · D. Ogawa ·
S. Okada · Y. Shikata · J. Wada · H. Makino

Erythromycin ameliorates renal injury via anti-inflammatory effects in experimental diabetic rats

Abstract *Aims/hypothesis:* Recent studies have shown that the inflammatory process is involved in the pathogenesis of diabetic nephropathy. Fourteen-membered ring macrolides, including erythromycin, have anti-inflammatory, as well as antibacterial effects. The aim of this study was to investigate the renoprotective effects of erythromycin in streptozotocin (STZ)-induced diabetic rats. *Methods:* STZ-induced diabetic rats were treated orally with erythromycin (5 mg/kg body weight) or vehicle every day for 8 weeks. To evaluate the effect of erythromycin treatment, we measured urinary albumin excretion, and examined the following in the kidney: histological changes, the expression of intercellular adhesion molecule-1 (ICAM-1), macrophage infiltration, and nuclear factor-kappa B (NF-κB) activity. *Results:* Erythromycin significantly reduced urinary albumin excretion without affecting blood glucose levels and blood pressure. Erythromycin also attenuated glomerular hypertrophy, mesangial expansion, macrophage infiltration and ICAM-1 expression in renal tissues. The expression of the gene encoding TGFB1 (also known as TGF-β1), type IV collagen protein production and NF-κB activity in renal tissues were increased in diabetic rats and reduced by erythromycin treatment. *Conclusions/interpretation:* Erythromycin prevented renal injuries without changes of blood glucose levels and blood pressure in experimental diabetic rats. These results suggest that the renoprotective effects of erythromycin are based on its anti-inflammatory effect via suppression of NF-κB activation. Modulation of microinflammation with erythromycin may provide a new approach for diabetic nephropathy.

A. Tone · K. Shikata (✉) · M. Sasaki · S. Ohga · K. Yozai ·
S. Nishishita · H. Usui · R. Nagase · D. Ogawa · S. Okada ·
Y. Shikata · J. Wada · H. Makino
Department of Medicine and Clinical Science,
Okayama University Graduate School of Medicine,
Dentistry and Pharmaceutical Sciences,
2-5-1 Shikata-cho,
Okayama, 700-8558, Japan
e-mail: shikata@md.okayama-u.ac.jp
Tel.: +81-86-2357235
Fax: +81-86-2225214

Introduction

Diabetic nephropathy is a leading cause of end-stage renal disease (ESRD) in many developed countries. It is well known that modulation of the renin–angiotensin system by ACE inhibitors (ACEI) and angiotensin II type 1 receptor antagonists (ARB) is effective in the treatment of diabetic nephropathy [1, 2]. Although ACEI and ARB play central roles in the therapy for diabetic nephropathy, additional new strategies are required because these drugs cannot completely prevent disease progression.

Several mechanisms contribute to the development of diabetic nephropathy. Glomerular hyperfiltration, which is noted in the early stage of diabetic nephropathy, causes glomerular injury in type 1 and type 2 diabetes [3]. Hyperglycaemia accelerates the accumulation of diacylglycerol and activates protein kinase C, resulting in overexpression of the genes encoding TGFB (also known as TGF-β) and extracellular matrix components in the mesangial cells and glomeruli [4]. Advanced glycation end-products stimulate mesangial cells and increase the production of extracellular matrix proteins such as type IV collagen [5, 6].

In addition to the pathways described above, recent studies have shown the involvement of inflammatory mechanisms in the pathogenesis of diabetic nephropathy. Furuta et al. [7] reported that macrophages infiltrate into renal tissues during the moderate stage of diabetic glomerulo-

sclerosis, suggesting that macrophages contribute to irreversible structural damage in type 2 diabetic patients. It has also been reported that glomerular and interstitial injury is associated with macrophage infiltration in both experimental type 1 and type 2 diabetes [8, 9]. Leucocyte infiltration into inflammatory sites and atherosclerotic lesions is mediated by cell adhesion molecules and chemokines such as chemokine (C–C motif) ligand 2 (CCL2) (also known as monocyte chemoattractant protein-1). We have recently demonstrated in a series of studies [10–12] that intercellular adhesion molecule-1 (ICAM-1) is upregulated and mediates macrophage infiltration in diabetic kidney tissues. We have also shown that ICAM-1 deficiency protects against renal injuries after induction of diabetes using ICAM-1 knockout mice [13]. Our recent studies strongly suggest that inflammatory mechanisms are involved in the pathogenesis of diabetic nephropathy and that ICAM-1 plays a central role in macrophage infiltration into diabetic kidney.

Fourteen-membered ring macrolides such as erythromycin have anti-inflammatory effects independent of their antibacterial effect in the fields of respiratory medicine and otolaryngology. Low-dose and long-term therapy with erythromycin, which reduces ICAM-1 expression in the airway epithelial cells and inhibits rhinovirus infection, is effective for chronic obstructive pulmonary disease, diffuse panbronchiolitis and chronic sinusitis [14–17]. It has also been reported that macrolides reduce the progression of bleomycin-induced lung injury in mice by inhibiting the induction of adhesion molecules, and neutrophil and macrophage migration into the airspace [18, 19].

The aim of this study was to investigate whether erythromycin, through its anti-inflammatory effect, protects against diabetic nephropathy in a model of streptozotocin (STZ)-induced diabetic rats.

Materials and methods

Animal model and experimental design

Protocol 1 Four-week-old Sprague–Dawley rats (CLER Japan, Tokyo, Japan) (mean body weight±SEM: 99.0± 2.0 g) were divided into the following four groups: (1) non-diabetic group (ND; n=6); (2) non-diabetic group treated with erythromycin (ND+EM; n=6); (3) STZ-induced diabetic group (DM; n=6); and (4) diabetic group treated with erythromycin (DM+EM; n=6). At the age of 5 weeks, rats chosen for the DM and DM+EM groups received intravenous injections of STZ (Sigma Chemical, St Louis, MO, USA) at 65 mg/kg body weight in citrate buffer (pH 4.5). Rats in the ND group received citrate buffer injections only. Starting from 7 days before the STZ injections, erythromycin (5 mg/kg body weight) in 4.2% ethanol was orally administrated with a conductor to rats in the ND+EM and DM+EM groups. This was done daily. Rats in the DM group received vehicle, administered in the same way.

All rats had free access to a standard diet and tap water. All procedures were performed according to the Guidelines for Animal Experimentation at the Okayama University Medical School, Japanese Government Animal Protection and Management Law (No.105), and Japanese Government Notification on Feeding and Safekeeping of Animals (No.6). Eight weeks after induction of diabetes in the DM and DM+EM groups, all rats were killed under ether anaesthesia and the kidneys were removed and weighed. Erythromycin base was donated by Dainippon Pharmaceutical (Osaka, Japan).

Protocol 2 An additional experiment was performed to assess glomerular haemodynamics at the early stage of diabetes. Diabetes was induced in the rats of the four groups as described in Protocol 1. Two weeks after induction of diabetes, all rats in this experiment were killed, and we measured creatinine clearance (Ccr) and kidney weight.

Metabolic data and functional measurements

Systolic blood pressure was measured by the tail-cuff method (Softron, Tokyo, Japan) at 4 and 8 weeks after induction of diabetes. HbA$_1$c, blood glucose and serum creatinine were assessed at 4 and 8 weeks after induction of diabetes. Urine samples were collected over a 24-h period in individual metabolic cages at 2, 4 and 8 weeks after induction of diabetes. HbA$_1$c, was measured by the HPLC method. Serum and urine creatinine were measured using enzymatic methods. The urinary albumin concentration in a 24-h urine collection was measured by nephelometry using anti-rat albumin antibody (ICN Pharmaceuticals, Aurora, OH, USA). Creatinine clearance (ml min^{-1} kg^{-1}) was calculated as [urinary creatinine volume/serum creatinine]/body weight. In Protocol 2, the above data were assessed at 2 weeks after induction of diabetes.

Assessment of kidney morphology by light microscopy

Renal tissues were fixed in 10% formalin and embedded in paraffin in routine fashion. Paraffin sections were cut at 4-μm thickness and stained with periodic acid–methenamine. To evaluate the glomerular size and mesangial matrix area, 20 randomly selected glomeruli per animal were examined. The glomerular tuft area was measured by manually tracing the glomerular tuft using PhotoShop version 6 (Adobe systems, San Jose, CA, USA) and analysed by Scion Image analysis software (Scion, Frederick, MD, USA). The mesangial matrix area was defined as the area positive for periodic acid–methenamine within the tuft area. The mesangial matrix index represented the ratio of mesangial matrix area to glomerular tuft area, as described previously [13].

Immunoperoxidase staining for macrophages

Infiltration of macrophages into the glomeruli was evaluated by immunoperoxidase staining using the ABC kit (Vector Laboratories, Burlingame, CA, USA) as described previously [9]. Briefly, frozen sections were cut at 4-μm thickness using a cryostat. Sections were incubated with a mouse monoclonal antibody against rat monocyte/macrophage (ED1) for 12 h at 4°C. The sections were then incubated with biotin-labelled goat anti-mouse IgG for 30 min at room temperature. Peroxidase activity was identified by reaction with 3,3′-diaminobenzidine. Mayer's haematoxylin was added as a counterstain. The average number of ED1-positive cells per glomerulus was calculated by counting the cells in 30 glomeruli per animal.

Immunofluorescence staining for ICAM-1 and type IV collagen

To evaluate the production of ICAM-1 and type IV collagen, immunofluorescence staining was performed as described previously [12, 20]. The frozen sections (4 μm) were stained with a monoclonal antibody against rat ICAM-1 (CD54) for 12 h at 4°C. The sections were then incubated with fluorescein-isothiocyanate-conjugated goat anti-mouse IgG for 30 min at room temperature. To characterise the change in mesangial matrix protein, rabbit anti-type IV collagen antibody was used for the primary reactions followed by a second reaction with fluorescein-isothiocyanate-conjugated goat anti-rabbit IgG (H+L).

Micrographic fluorescence photos were obtained using a laser-scanning confocal microscope (LSM-510; Carl Zeiss, Jena, Germany). The immunofluorescence intensity of ICAM-1 and type IV collagen was quantified by the modified method, as described previously [20]. In brief, colour images were obtained as TIFF target image files from the LSM-510. The brightness of each image file was uniformly enhanced by Photoshop (Adobe), followed by analysis using image analysis software (Scion). TIFF target image files were inverted and opened in grey scale mode. The ICAM-1 index and type IV collagen index were calculated using the formula: positive area mean density × positive area (μm^2)/glomerular total area (μm^2), where the staining density is indicated by a number from 0 to 256 in grey scale. We evaluated 30 glomeruli per animal.

Quantitative analysis of Tgfb1 and Ccl2 mRNA by real-time RT-PCR

Total RNA was extracted from each specimen of renal cortex using the RNeasy kit (Qiagen, Valencia, CA, USA). Single-strand complementary DNA was synthesised from the extracted RNA using a reverse transcription-PCR kit (Perkin Elmer, Foster City, CA, USA) according to the manufacturer's instructions. To evaluate mRNA expression of *Tgfb1*, *Ccl2* and *Actb* (which encodes β-actin) in renal cortex, quantitative real-time RT-PCR was performed using a Light Cycler and LightCycler-FastStart SYBR Green 1 (Roche Diagnostics, Tokyo, Japan). After the addition of primers (final concentration: 0.3 μmol/l), $MgCl_2$ (3 mmol/l) and template DNA to the master mix, 45 cycles of denaturation (95°C for 10 s), annealing (60°C for 15 s) and extension (72°C for 10 s) were performed. To determine the

Table 1 Time course of metabolic data and functional measurements after induction of diabetes mellitus
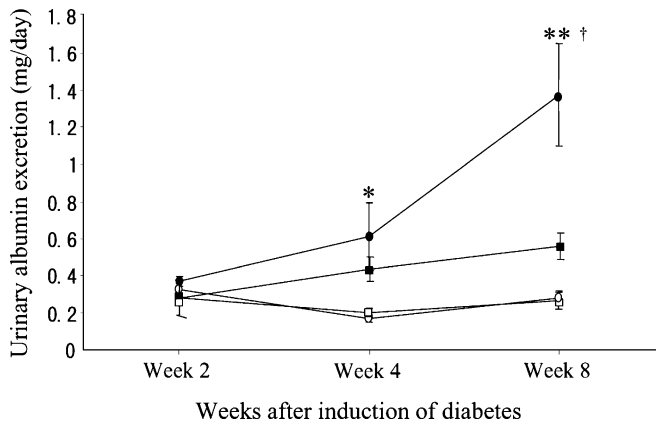
Data are means±SEM of six rats of each group
[a]$p<0.0001$ vs ND; [b]$p<0.0001$ vs ND+EM; [c]$p<0.005$ vs ND; [d]$p<0.005$ vs ND+EM; [e]$p<0.01$ vs ND
Ccr Creatinine clearance

	Non-diabetic rats (ND)	Non-diabetic rats treated with erythromycin (ND+EM)	Diabetic rats (DM)	Diabetic rats treated with erythromycin (DM+EM)
HbA$_1$c (%)				
Week 4	3.2±0.15	2.6±0.05	10.7±0.32[a,b]	10.0±0.33[a,b]
Week 8	3.8±0.14	3.4±0.07	14.1±0.21[a,b]	13.4±0.21[a,b]
Body weight (g)				
Week 2	237±9.4	240±4.0	227±9.8	246±11.4
Week 4	356±5.7	360±4.4	277±18.7[c,d]	288±14.7[d,e]
Week 8	517±8.6	505±4.4	304±29.7[a,b]	274±17.6[a,b]
Relative kidney weight (g/kg body weight)				
Week 8	3.2±0.13	3.0±0.06	5.5±0.25[a,b]	6.1±0.18[a,b]
Systolic blood pressure (mm Hg)				
Week 4	118.3±2.8	111.2±7.8	121.8±2.6	118.5±4.2
Week 8	129.7±2.8	114.9±4.3	119.5±5.7	118.2±6.8
Serum creatinine (μmol/l)				
Week 4	13.4±1.17	15.3±0.54	15.3±1.06	12.8±1.80
Week 8	22.0±1.67	23.6±0.88	19.0±1.84	21.7±1.60
Ccr (ml min^{-1}kg^{-1})				
Week 4	12.4±0.53	11.9±0.64	11.0±1.34	12.2±2.58
Week 8	8.9±0.64	7.8±0.26	7.0±0.75	7.1±0.28

Fig. 1 Time course of changes in urinary albumin excretion in non-diabetic rats (ND group; *open circles*), non-diabetic rats with erythromycin (ND+EM group; *open squares*), untreated diabetic rats (DM group; *filled circles*) and diabetic rats treated with erythromycin (DM+EM group; *filled squares*). Although urinary albumin excretion in the DM group progressively increased compared with the ND and ND+EM groups, it was significantly reduced by treatment with erythromycin at week 8. Data are means±SEM of six rats in each group. *$p<0.05$ vs ND group and ND+EM group; **$p<0.01$ vs DM+EM group; †$p<0.001$ vs ND group and ND+EM group

specificity of each primer set, melting curve analysis was performed after the completion of PCR amplification.

Accumulated levels of fluorescence were analysed by the fit-point method after melting curve analysis. The mRNA level of *Tgfb1* and *Ccl2* was normalised with a house-keeping gene (*Actb*) in each sample by calculating the relative expression ratio. For amplification of the complementary DNA, the following oligonucleotide primers specific for rat *Tgfb1* (GenBank; X52498), *Ccl2* (GenBank; M57441) and *Actb* (GenBank; NM_031144) were used: *Tgfb1*, sense 5′-GCAACAACGCAATCTAT GAC-3′, antisense 5′-CCTGTATTCCGTCTCCTT-3′; *Ccl2*, sense 5′-TCGGCTGGAGAACTACAAG -3′, antisense 5′-C TGAAGTCCTTAGGGTTGATG-3′; *Actb*, sense 5′-CCTG TATGCCTCTGGTCGTA-3′, antisense 5′-CCATCTCTT GCTCGAAGTCT-3′ (Nihon Gene Research Labs, Sendai, Japan). Each experiment was performed twice.

Electrophoretic mobility shift assay

Tissue extracts and electrophoretic mobility shift assay for the transcription factor nuclear factor-κB (NF-κB) were performed as previously described [20]. In brief, frozen renal cortex was minced and suspended in 1 ml of TBS buffer (25 mmol/l Tris–HCl [pH 7.4], 130 mmol/l NaCl and 5 mmol/l KCl) and homogenised. The pellet was re-suspended in 1 ml of buffer A (10 mmol/l HEPES [pH 7.9], 10 mmol/l KCl, 0.1 mmol/l EDTA [pH 7.5], 0.1 mmol/l EGTA [pH 7.5], 1 mmol/l phenylmethylsulfonyl fluoride and 1 mmol/l dithiothreitol [DTT]) and incubated on ice for 20 min. Then, 100 μl of 10% Nonidet P-40 was added and vigorously vortexed. The nuclear fraction was collected by centrifugation and was resuspended in 100 μl of buffer B (20 mmol/l HEPES [pH 7.9], 400 mmol/l NaCl, 1 mmol/l EDTA [pH 7.5], 1 mmol/l EGTA [pH 7.5], 1 mmol/l phenylmethylsulfonyl fluoride and 1 mmol/l DTT).

For the electrophoretic mobility shift assay, the following oligonucleotide containing an NF-κB binding site was used: 5′-AGTTGAGGGGACTTTCCCAGGC-3′ (Santa Cruz Biotechnology, Santa Cruz, CA, USA). A mutant motif with G to C substitution (5′-AGTTGAGGCGAC TTTCCCAGGC-3′; Santa Cruz Biotechnology) served as a control. The consensus oligonucleotide was labelled with [γ-^{32}P] ATP (Amersham Biosciences, Piscataway, NJ, USA) using T4 Poly-nucleotide kinase (Promega, Madison, WI, USA). Nuclear extract (45 μg) was incubated with
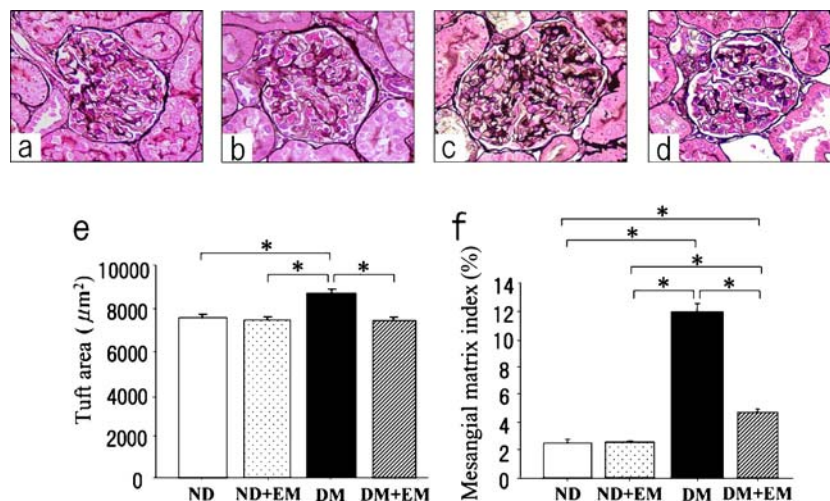
Fig. 2 Periodic acid–methenamine staining in glomeruli from a non-diabetic rat (**a**), a non-diabetic rat with erythromycin (**b**), an untreated diabetic rat (**c**) and an erythromycin-treated diabetic rat (**d**) (*magnification* ×400). Glomerular size (*tuft area*) in untreated diabetic rats (DM) (**e**) was significantly larger than in the other three groups.

Although mesangial matrix was significantly greater in the DM group than in the ND and ND+EM groups, treatment with erythromycin significantly reduced mesangial expansion by 60.5% (**f**). Data are means±SEM values of six rats in each group. *$p<0.0001$

1 ng of $[\gamma\text{-}^{32}P]$ ATP ^{32}P-labelled oligonucleotide in 20 µl binding buffer (10 mmol/l Tris–HCl [pH 7.5], 50 mmol/l NaCl, 0.5 mmol/l EDTA, 0.5 mmol/l DTT, 1 mmol/l MgCl$_2$, 4% glycerol and 50 mg/ml poly dI–dC) for 20 min at room temperature. Individual samples were then electrophoresed on a 4% polyacrylamide gel. After electrophoresis, the gel was dried and exposed to an imaging plate (Fujifilm, Tokyo, Japan). The autoradiogram was read by a FUJIX BAS-2000 (Fujifilm) and the relative intensity of the autoradiogram was determined using image analysis software (Scion). To assess the specificity of the reaction, a competition assay was performed in which 100-fold excess unlabelled NF-κB consensus sequences were added to the binding reaction 20 min prior to the radiolabelled NF-κB oligonucleotide. Each experiment was performed three times. For supershift/antibody competition assay, antibody against the p65 subunit (Active Motif, Tokyo, Japan) was incubated with nuclear extract for 20 min at 4°C before the binding reaction.

Antibodies

The primary antibodies used were mouse anti-rat monocyte/macrophage (ED1) monoclonal antibody (Serotec, Oxford, UK), purified mouse anti-rat ICAM-1 (CD54) monoclonal antibody (Seikagaku, Tokyo, Japan) and rabbit anti-mouse type IV collagen antibody (LSL, Tokyo, Japan).

The secondary antibodies were biotin-labelled goat anti-mouse IgG (Jackson Immunoresearch Laboratories, West Grove, PA, USA), fluorescein-isothiocyanate-conjugated goat anti-mouse IgG (Jackson Immunoresearch Laboratories) and fluorescein-isothiocyanate-conjugated goat anti-rabbit IgG (H+L) (Zymed laboratories, San Francisco, CA, USA).

Statistical analysis

All data are expressed as the mean±SEM. Differences between groups were examined for statistical significance using ANOVA followed by Scheffé's test. A p value of less than 0.05 denoted the presence of a statistically significant difference.

Results

Protocol 1

Time course of metabolic data and functional measurements

Changes in metabolic data and functional measurements are shown in Table 1. There was no significant difference in HbA$_1$c, or body weight between the DM and DM+EM

Fig. 3 ICAM-1 production (**a**–**d**) and macrophage infiltration (**e**–**h**). Kidney tissues were taken from non-diabetic rats (**a**, **e**), non-diabetic rats treated with erythromycin (**b**, **f**), untreated diabetic rats (**c**, **g**) and erythromycin-treated diabetic rats (**d**, **h**). The production of ICAM-1 protein and infiltration of ED-1-positive cells (*macrophage*: arrows) into glomeruli were predominantly observed in glomeruli from untreated diabetic rats and were significantly inhibited in erythromycin-treated diabetic rats (*magnification* ×400). Immunofluorescence intensity for ICAM-1 (ICAM-1 index) (**i**) and the number (**j**) of ED-1-positive cells (*macrophages*). Data are means±SEM values of six rats in each group. *$p<0.0001$; **$p<0.01$; †$p<0.05$
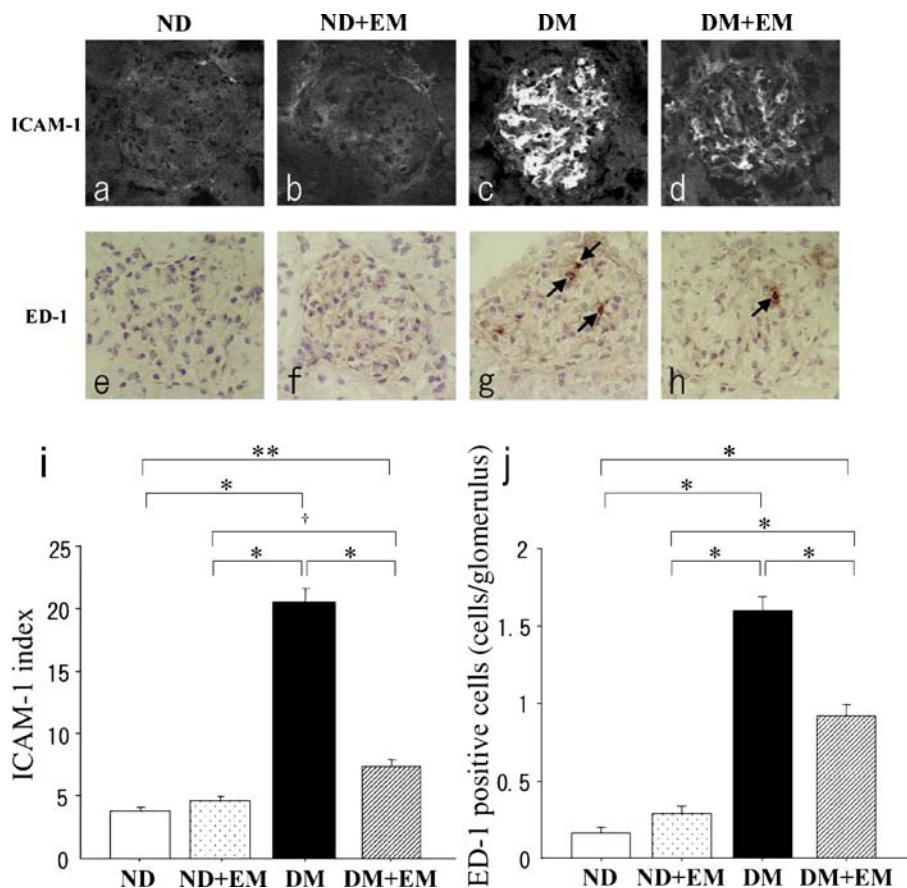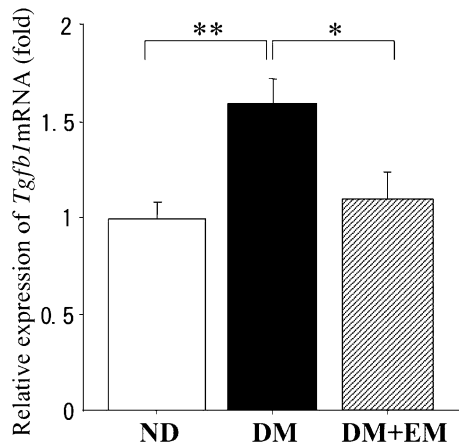
Fig. 4 Expression of *Tgfb1* mRNA in renal cortex estimated by quantitative real-time RT-PCR. The mRNA level of *Tgfb1* was normalised to the level of *Actb* mRNA in each sample by calculating the relative expression ratio. Data are means±SEM of 6 rats in each group. *$p<0.05$; **$p<0.01$

groups. While relative kidney weights in the DM and DM+EM groups were significantly higher than in the ND and ND+EM groups, there was no significant difference between the DM and DM+EM groups. There were no significant differences in systolic blood pressure, serum creatinine and Ccr among the four groups at weeks 4 and 8.

Urinary albumin excretion

Urinary albumin excretion after induction of diabetes is shown in Fig. 1. Urinary albumin excretion in untreated diabetic rats (DM group) progressively increased at weeks 4 and 8 compared with non-diabetic rats (ND group) and non-diabetic rats treated with erythromycin (ND+EM group). However, the treatment with erythromycin significantly

reduced urinary albumin excretion by 59.5% at week 8 ($p<0.01$).

Kidney morphology

Periodic acid–methenamine staining in glomeruli from each group is shown in Fig. 2a-d. Glomerular hypertrophy and mesangial matrix expansion were evaluated by calculating glomerular size (tuft area) and mesangial matrix index. The tuft area was significantly larger in the DM group than in the other three groups ($p<0.0001$) (ND vs ND+ EM vs DM vs DM+EM: 7605±156 vs 7340±136 vs 8784± 175 vs 7460±145 μm²; Fig. 2e). Although the mesangial matrix was significantly greater in the DM group than in the ND and ND+EM groups, erythromycin treatment significantly reduced mesangial expansion by 60.5% (Fig. 2f).

ICAM-1 production and macrophage infiltration into glomeruli

Immunofluorescence staining for ICAM-1 in glomeruli and immunoperoxidase staining for ED-1 (macrophages) is shown in Fig. 3a–h. The ICAM-1 index was calculated to quantify ICAM-1 immunofluorescence intensity. The production of ICAM-1 protein in the DM group showed a nearly five-fold increase compared with the ND and ND+ EM groups and exhibited a 64% reduction by the treatment with erythromycin (Fig. 3i). The number of ED-1-positive cells (macrophages) in glomeruli was significantly higher in untreated diabetic rats than in non-diabetic rats and non-diabetic rats treated with erythromycin. The infiltration of macrophages was significantly suppressed by treatment with erythromycin (ND vs ND+EM vs DM vs DM+EM: 0.2±0.03 vs 0.3±0.04 vs 1.6±0.08 vs 0.9±0.07 cells/ glomerulus; Fig. 3j).

Fig. 5 Quantitative analysis of type IV collagen in glomeruli from non-diabetic rats (**a**), untreated diabetic rats (**b**) and diabetic rats treated with erythromycin (**c**). The immunofluorescence intensity of type IV collagen was estimated using the same method as for the ICAM-1 index (**d**). The intensity of type IV collagen in glomeruli was significantly higher in the DM group than in the ND group, the increase in type IV collagen production was markedly inhibited by treatment with erythromycin (DM+EM). Data are mean±SEM values of six rats in each group. *$p<0.0001$; **$p<0.005$
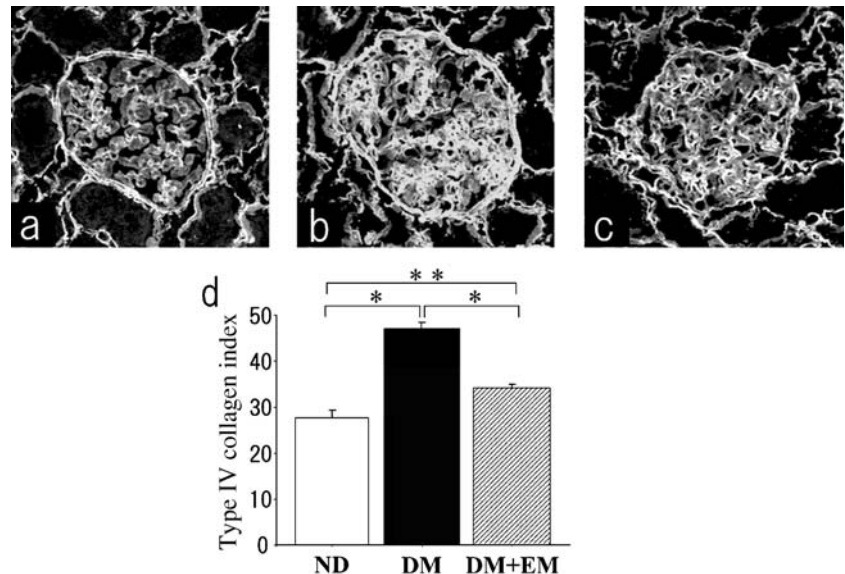
Fig. 6 Electrophoretic mobility shift assay for NF-κB (**a**). ND, non-diabetic rats; DM, untreated diabetic rats; DM+EM, erythromycin-treated diabetic rats. Lanes 1–3, NF-κB activation. Lanes 4 and 5, specificity of NF-κB DNA binding. Lane 4, without nuclear extract; lane 5, pretreated with excess cold mutant NF-κB. Lane 6, pretreated with excess cold NF-κB. **b** Results of densitometric analysis of NF-κB activation in the kidneys. Data are expressed as mean±SEM values of six rats in each group. *$p<0.01$, **$p<0.005$
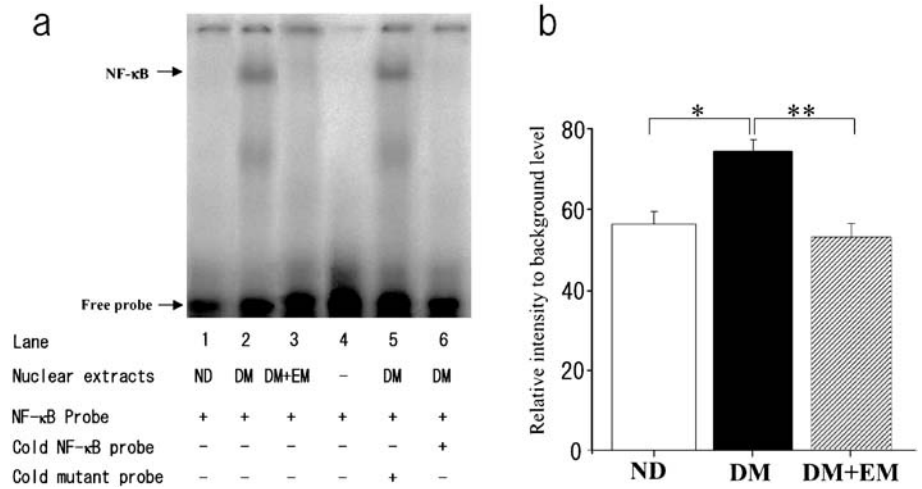
Expression of Tgfb1 mRNA and type IV collagen protein in renal tissue

To investigate the inhibitory effect of erythromycin on *Tgfb1* mRNA expression in renal cortex, quantitative real-time RT-PCR was performed. The level of *Tgfb1* mRNA was normalised to the level of *Actb* mRNA in each sample by calculating the relative expression ratio. *Tgfb1* mRNA expression in untreated diabetic rats was 1.6-fold higher than in non-diabetic rats ($p<0.01$). Erythromycin treatment reduced the increase of *Tgfb1* mRNA expression by 83.5%, $p<0.05$ vs DM group) (Fig. 4). Melting curve analysis confirmed the specificity of the *Tgfb1* and *Actb* PCR products (data not shown).

Immunofluorescence staining for type IV collagen in glomeruli is shown in Fig. 5a–c. To quantify the intensity of type IV collagen expression, the immunofluorescence intensity was calculated using the same method as for the ICAM-1 index. The intensity of type IV collagen in glomeruli was significantly higher in the DM group than in the ND group; the intensity in the DM+EM group was markedly lower than in the DM group (Fig. 5d).

NF-κB activation

The activation of NF-κB DNA binding activity, which is involved in gene expression for a variety of inflammatory mediators and adhesion molecules, was analysed by electrophoretic mobility shift assay (Fig. 6a). NF-κB DNA binding activity is shown as intensity relative to background level (lane 6). NF-κB activation was 1.3-fold higher in the kidneys of untreated diabetic rats than in non-diabetic rats and was significantly reduced by treatment with erythromycin (Fig. 6b).

Activation of p65 subunit

Supershift/antibody competition assays were performed to evaluate the specificity of the NF-κB components. Super-

shift assays demonstrated that an antibody directed against the p65 subunit supershifted NF-κB binding (Fig. 7).

Ccl2 gene expression in renal tissue

The expression of *Ccl2*, known to be NF-κB-dependent and one of the major mediators of macrophage recruitment,
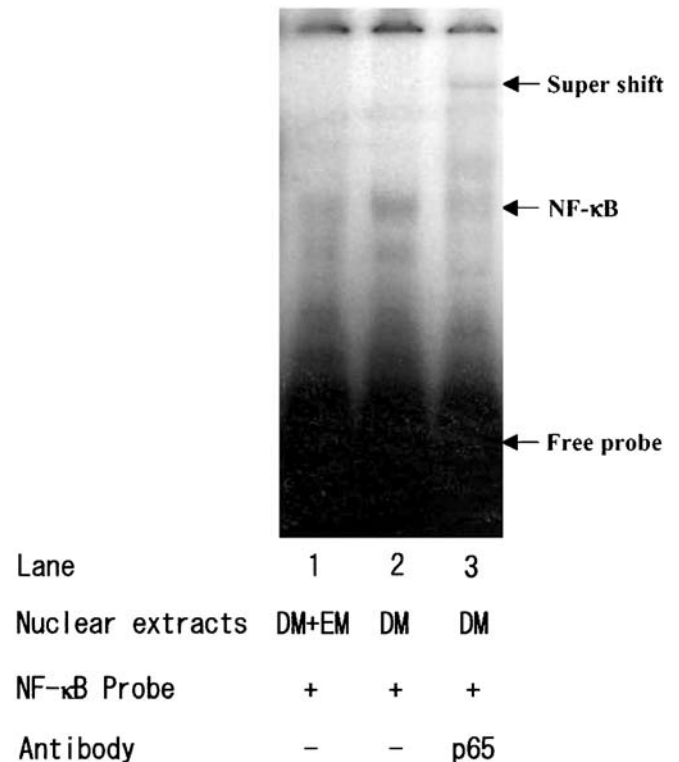
Fig. 7 The specificity of the NF-κB components evaluated by supershift/antibody competition assay. Lane 1, nuclear extracts from the DM+EM group; lane 2, nuclear extracts from the DM group without antibody; lane 3, an antibody against the p65 subunit was added with the nuclear extracts from the DM group. The gel shown is representative of five separate experiments
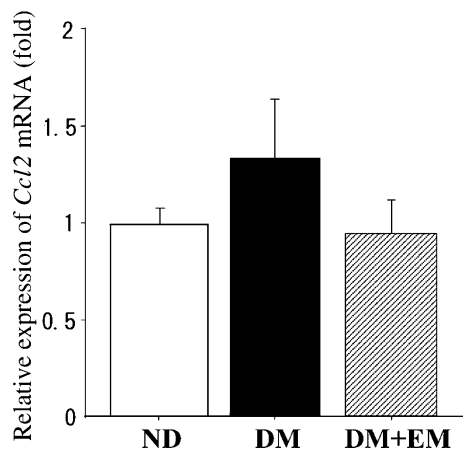
Fig. 8 *Ccl2* expression in renal tissue estimated by quantitative real-time RT-PCR. The mRNA level of *Ccl2* was normalised to the level of*Actb* mRNA in each sample by calculating the relative expression ratio

was evaluated by quantitative real-time RT-PCR. The renal expression of *Ccl2* paralleled the changes in NF-κB and renal macrophage infiltration, but were not statistically significant (Fig. 8). Melting curve analysis confirmed the specificity of the *Ccl2* PCR products (data not shown).

Protocol 2

To assess glomerular haemodynamic changes in earlier stage of diabetes in this experimental model, an additional experiment was performed 2 weeks after induction of diabetes. Metabolic data and functional measurements are shown in Table 2. At 2 weeks after induction of diabetes, Ccr was significantly higher in the DM and DM+EM groups than in the ND and ND+EM groups. However, the level of Ccr was not significantly different between the DM and DM+EM groups. Relative kidney weights in the DM and DM+EM groups were significantly higher than in the ND and ND+EM groups, although there were no significant differences between the DM and DM+EM groups.

There were no significant differences in systolic blood pressure and serum creatinine among the four groups and the HbA$_1$c level was not significantly different between the DM and DM+EM groups.

Discussion

The major findings of the present study were that continuous erythromycin treatment prevented renal injuries and macrophage infiltration into renal tissue through suppression of ICAM-1 production without change of blood glucose level and blood pressure in experimental diabetic rats. The renoprotective effect of erythromycin may result from its anti-inflammatory effect via inactivation of NF-κB, which is one of the major transcription factors for ICAM-1, proinflammatory cytokines [21] and chemokines [22–24]. Supershift assays suggested that the activation of p65 subunit contributes to the pathogenesis of the inflammatory mechanisms in diabetic nephropathy.

Lee et al. [24] reported that the active subunit of NF-κB, p65, was elevated in the kidney of diabetic rats and associated with *Ccl2* expression and macrophage infiltration. Our results are consistent with their report. Although we did not detect the significant change in renal *Ccl2* expression in the ND, DM and DM+EM groups, *Ccl2*, which is NF-κB-dependent, might also contribute to the inflammatory processes in diabetic kidneys.

ACEI and ARB are known to play central roles in the treatment of diabetic nephropathy, mainly by improving glomerular haemodynamic abnormalities. Recently, it was reported that angiotensin II induces cytokine/chemokine production and NF-κB activation in the kidney, and that ACEI and ARB, which are known to reduce TGFB up-regulation, ameliorate a series of inflammatory process [22, 25–27]. It has also been reported that the renoprotective effects of ARB are related to inhibition of the NF-κB-dependent pathway in modulating macrophage infiltration in diabetic nephropathy [24]. Thus, the effects of ACEI and ARB on diabetic nephropathy may at least partly be related to anti-inflammatory actions.

We have previously demonstrated that ICAM-1 is expressed on glomerular endothelial cells and peritubular capillaries and promotes the infiltration of macrophages into kidney in diabetic patients and animal models of diabetes [10–12]. Furthermore, we induced diabetes in ICAM-1 knock-out mice and examined the change of renal injuries. ICAM-1 deficiency resulted in suppression of macrophage infiltration into renal tissue, as well as of TGFB and type IV collagen production and urinary albumin excretion, as compared with diabetic wild-type mice [13].

Table 2 Metabolic data and functional measurements at 2 weeks after induction of diabetes

	Non-diabetic rats (ND)	Non-diabetic rats treated with erythromycin (ND+EM)	Diabetic rats (DM)	Diabetic rats treated with erythromycin (DM+EM)
HbA$_1$c (%)	2.4±0.13	2.2±0.09	5.0±0.34[a,b]	4.9±0.24[a,b]
Systolic blood pressure (mm Hg)	112.1±7.7	113.4±5.3	109.6±4.5	122.4±5.7
Serum creatinine (μmol/l)	12.7±1.18	13.3±1.27	13.0±0.59	13.9±0.44
Relative kidney weight (g/kg body weight)	4.7±0.25	4.4±0.16	6.0±0.26[c,d]	5.9±0.19[c,d]
Ccr (ml min^{-1}kg^{-1})	11.4±0.81	11.7±0.27	14.6±0.74[c,e]	15.0±0.64[c,e]

Data are means±SEM of six rats from each group
[a]$p<0.0001$ vs ND; [b]$p<0.0001$ vs ND+EM; [c]$p<0.01$ vs ND; [d]$p<0.001$ vs ND+EM; [e]$p<0.05$ vs ND+EM

Some other reports show the correlation between diabetes and inflammatory phenomena in the kidney. High glucose activates the TGFB-dependent Smad signalling pathway to stimulate collagen synthesis in diabetic kidney [28]. Gruden and co-workers [29] reported that mechanical stretch induces CCL2 production via the NF-κB-dependent pathway in human mesangial cells. Mezzano et al. [30] reported that the activation of NF-κB and chemokines such as CCL2 and RANTES (regulated upon activation, normal T expressed and secreted) was strongly upregulated in renal tissues of human diabetic nephropathy. Moreover, high glucose upregulates peroxisome proliferator-activated receptor-γ (PPAR-γ), and PPAR-γ agonists exert anti-fibrotic, anti-proliferative and anti-inflammatory effects in renal proximal tubular cells under high glucose conditions by attenuating the increase in activator protein-1, TGFB1 and the downstream production of the extracellular matrix protein [31, 32]. These data also suggest that inflammatory mechanisms are involved in the progression of diabetic nephropathy.

On the other hand, mechanical stretch and high glucose directly stimulate *Tgfb1* expression and TGFB1 production in cultured mesangial cells, resulting in collagen accumulation [33–36]. These results indicate that metabolic and haemodynamic changes may also induce extracellular matrix accumulation independently of inflammation in the development of diabetic glomerulosclerosis.

We have recently shown that statin treatment downregulates ICAM-1 expression by inhibiting NF-κB activation, and protects from renal damage in experimental diabetic rats [20]. Utimura and co-workers [37] have also reported that mycophenolate mofetil attenuated renal damage in streptozotocin-induced diabetic rats by its anti-inflammatory effects. These data suggest that inflammatory mechanisms might be a new target in the therapy of diabetic nephropathy.

Recently, another study using mice with bleomycin-induced lung injury [18] showed that macrolides inhibited the expression of mRNA transcripts of the genes for vascular adhesion molecule-1 and ICAM-1 in lung tissues and attenuated the migration of inflammatory cells, especially neutrophils and macrophages, into air spaces. With respect to the direct effect on vascular endothelial cells, Enomoto et al. [38] reported that erythromycin directly reduced ICAM-1 expression that was upregulated by TNF-α stimulation using cultured vascular endothelial cells. These data support the results of the present study. On the other hand, it was reported that macrolides directly act on monocytes or macrophages and inhibit the production of inflammatory cytokines such as IL-1, IL-8 and TNF-α in vitro [39, 40]. It was also reported that macrolides, including erythromycin, inhibit NF-κB activation in mononuclear cells and macrophages [41–43]. Kikuchi and colleagues [44] reported that clarithromycin suppressed lipopolysaccharide-induced IL-8 production in human peripheral monocytes and in the human monocytic leukaemia cell line THP-1, through suppression of activator protein-1, and NF-κB transcription factors. These in vitro findings suggest that in our study,

erythromycin might have directly acted on macrophages as well as on glomerular endothelial cells.

In our study, erythromycin treatment prevented glomerular hypertrophy in diabetic rats. The treatment with erythromycin did not change elevated Ccr in diabetic rats at 2 weeks after induction of diabetes, indicating that erythromycin does not affect glomerular haemodynamic changes. Therefore, we suggest that erythromycin does not reduce glomerular size by modulating haemodynamics, but rather by suppressing mesangial cell hypertrophy and extracellular matrix expansion, which is mainly composed of type IV collagens. It has previously [45] been shown that the early characteristic features of diabetic nephropathy, including glomerular hypertrophy and increased matrix synthesis, are largely mediated by increased TGFB activity in the kidney. The present study suggests that erythromycin treatment reduces the increase of type IV collagens and mesangial matrix expansion by modulating the inflammatory processes and through that suppressing TGFB activity.

In conclusion, in our present study erythromycin reduced ICAM-1 production and macrophage infiltration through suppression of NF-κB activation. The mechanism is partly similar to that in chronic obstructive pulmonary disease, diffuse panbronchiolitis and sinusitis. Low-dose and long-term administration of erythromycin is in common clinical use, and the safety of the therapy is established. Thus, modulation of inflammation with erythromycin might provide a new approach for diabetic nephropathy.

References

1. Parving HH, Lehnert H, Brochner-Mortensen J, Gomis R, Andersen S, Arner P (2001) The effect of irbesartan on the development of diabetic nephropathy in patients with type 2 diabetes. N Engl J Med 345:870–878
2. Lewis EJ, Hunsicker LG, Bain RP, Rohde RD (1993) The effect of angiotensin-converting-enzyme inhibition on diabetic nephropathy. The Collaborative Study Group. N Engl J Med 329:1456–1462
3. Hiragushi K, Sugimoto H, Shikata K et al (2001) Nitric oxide system is involved in glomerular hyperfiltration in Japanese normo- and micro-albuminuric patients with type 2 diabetes. Diabetes Res Clin Pract 53:149–159
4. Koya D, Jirousek MR, Lin YW, Ishii H, Kuboki K, King GL (1997) Characterization of protein kinase C beta isoform activation on the gene expression of transforming growth factor-beta, extracellular matrix components, and prostanoids in the glomeruli of diabetic rats. J Clin Invest 100:115–126
5. Pugliese G, Pricci F, Romeo G et al (1997) Upregulation of mesangial growth factor and extracellular matrix synthesis by advanced glycation end products via a receptor-mediated mechanism. Diabetes 46:1881–1887
6. Yang CW, Vlassara H, Peten EP, He CJ, Striker GE, Striker LJ (1994) Advanced glycation end products up-regulate gene expression found in diabetic glomerular disease. Proc Natl Acad Sci U S A 91:9436–9440

7. Furuta T, Saito T, Ootaka T et al (1993) The role of macrophages in diabetic glomerulosclerosis. Am J Kidney Dis 21:480–485

8. Sassy-Prigent C, Heudes D, Mandet C et al (2000) Early glomerular macrophage recruitment in streptozotocin-induced diabetic rats. Diabetes 49:466–475

9. Chow F, Ozols E, Nikolic-Paterson DJ, Atkins RC, Tesch GH (2004) Macrophages in mouse type 2 diabetic nephropathy: correlation with diabetic state and progressive renal injury. Kidney Int 65:116–128

10. Hirata K, Shikata K, Matsuda M et al (1998) Increased expression of selectins in kidneys of patients with diabetic nephropathy. Diabetologia 41:185–192

11. Miyatake N, Shikata K, Sugimoto H et al (1998) Intercellular adhesion molecule 1 mediates mononuclear cell infiltration into rat glomeruli after renal ablation. Nephron 79:91–98

12. Sugimoto H, Shikata K, Hirata K et al (1997) Increased expression of intercellular adhesion molecule-1 (ICAM-1) in diabetic rat glomeruli: glomerular hyperfiltration is a potential mechanism of ICAM-1 upregulation. Diabetes 46:2075–2081

13. Okada S, Shikata K, Matsuda M et al (2003) Intercellular adhesion molecule-1-deficient mice are resistant against renal injury after induction of diabetes. Diabetes 52:2586–2593

14. Kadota Ji J (1996) Non-antibiotic effect of antibiotics. Clin Microbiol Infect 1(Suppl 2):S20–S22

15. Suzuki T, Yanai M, Yamaya M et al (2001) Erythromycin and common cold in COPD. Chest 120:730–733

16. Yamaya M, Sasaki H (2003) Rhinovirus and asthma. Viral Immunol 16:99–109

17. Miyajima M, Suga M, Nakagawa K, Ito K, Ando M (1999) Effects of erythromycin on experimental extrinsic allergic alveolitis. Clin Exp Allergy 29:253–261

18. Li Y, Azuma A, Takahashi S et al (2002) Fourteen-membered ring macrolides inhibit vascular cell adhesion molecule 1 messenger RNA induction and leukocyte migration: role in preventing lung injury and fibrosis in bleomycin-challenged mice. Chest 122:2137–2145

19. Azuma A, Furuta T, Enomoto T et al (1998) Preventive effect of erythromycin on experimental bleomycin-induced acute lung injury in rats. Thorax 53:186–189

20. Usui H, Shikata K, Matsuda M et al (2003) HMG-CoA reductase inhibitor ameliorates diabetic nephropathy by its pleiotropic effects in rats. Nephrol Dial Transplant 18:265–272

21. Guijarro C, Egido J (2001) Transcription factor-kappa B (NF-kappa B) and renal disease. Kidney Int 59:415–424

22. Kato S, Luyckx VA, Ots M et al (1999) Renin–angiotensin blockade lowers MCP-1 expression in diabetic rats. Kidney Int 56:1037–1048

23. Ueda A, Ishigatsubo Y, Okubo T, Yoshimura T (1997) Transcriptional regulation of the human monocyte chemoattractant protein-1 gene. Cooperation of two NF-kappa B sites and NF-kappa B/Rel subunit specificity. J Biol Chem 272:31092–31099

24. Lee FT, Cao Z, Long DM et al (2004) Interactions between angiotensin II and NF-kappa B-dependent pathways in modulating macrophage infiltration in experimental diabetic nephropathy. J Am Soc Nephrol 15:2139–2151

25. Mezzano SA, Ruiz-Ortega M, Egido J (2001) Angiotensin II and renal fibrosis. Hypertension 38:635–638

26. Benigni A, Remuzzi G (2001) How renal cytokines and growth factors contribute to renal disease progression. Am J Kidney Dis 37:S21–S24

27. Ruiz-Ortega M, Lorenzo O, Ruperez M, Blanco J, Egido J (2001) Systemic infusion of angiotensin II into normal rats activates nuclear factor-kappa B and AP-1 in the kidney: role of AT(1) and AT(2) receptors. Am J Pathol 158:1743–1756

28. Li JH, Huang XR, Zhu HJ, Johnson R, Lan HY (2003) Role of TGF-beta signalling in extracellular matrix production under high glucose conditions. Kidney Int 63:2010–2019

29. Gruden G, Setti G, Hayward A et al (2005) Mechanical stretch induces monocyte chemoattractant activity via an NF-kappa-B-dependent monocyte chemoattractant protein-1-mediated pathway in human mesangial cells: inhibition by rosiglitazone. J Am Soc Nephrol 16:688–696

30. Mezzano S, Aros C, Droguett A et al (2004) NF-kappa B activation and overexpression of regulated genes in human diabetic nephropathy. Nephrol Dial Transplant 19:2505–2512

31. Panchapakesan U, Pollock CA, Chen XM (2004) The effect of high glucose and PPAR-gamma agonists on PPAR-gamma expression and function in HK-2 cells. Am J Physiol Renal Physiol 287:F528–F534

32. Panchapakesan U, Sumual S, Pollock CA, Chen X (2005) PPAR gamma agonists exert antifibrotic effects in renal tubular cells exposed to high glucose. Am J Physiol Renal Physiol 10 (in press)

33. Hoffman BB, Sharma K, Zhu Y, Ziyadeh FN (1998) Transcriptional activation of transforming growth factor-beta1 in mesangial cell culture by high glucose concentration. Kidney Int 54:1107–1116

34. Riser BL, Cortes P, Yee J et al (1998) Mechanical strain- and high glucose-induced alterations in mesangial cell collagen metabolism: role of TGF-beta. J Am Soc Nephrol 9:827–836

35. Yasuda T, Kondo S, Homma T, Harris RC (1996) Regulation of extracellular matrix by mechanical stress in rat glomerular mesangial cells. J Clin Invest 98:1991–2000

36. Ishida T, Haneda M, Maeda S, Koya D, Kikkawa R (1999) Stretch-induced overproduction of fibronectin in mesangial cells is mediated by the activation of mitogen-activated protein kinase. Diabetes 48:595–602

37. Utimura R, Fujihara CK, Mattar AL et al (2003) Mycophenolate mofetil prevents the development of glomerular injury in experimental diabetes. Kidney Int 63:209–216

38. Enomoto F, Kin R, Kataoka T et al (2003) Modulation of neutrophil adhesion to vascular endothelial cells in rat experimental otitis media treated with a macrolide. Auris Nasus Larynx 30:247–251

39. Iino Y, Toriyama M, Kudo K, Natori Y, Yuo A (1992) Erythromycin inhibition of lipopolysaccharide-stimulated tumor necrosis factor alpha production by human monocytes in vitro. Ann Otol Rhinol Laryngol (Suppl) 157:16–20

40. Fujii T, Kadota J, Morikawa T et al (1996) Inhibitory effect of erythromycin on interleukin 8 production by 1 alpha,25-dihydroxyvitamin D3-stimulated THP-1 cells. Antimicrob Agents Chemother 40:1548–1551

41. Ren W, Li XH, Chen BD, Wooley PH (2004) Erythromycin inhibits wear debris-induced osteoclastogenesis by modulation of murine macrophage NF-kappa B activity. J Orthop Res 22:21–29

42. Wallwork B, Coman W, Mackay-Sim A, Cervin A (2004) Effect of clarithromycin on nuclear factor-kappa B and transforming growth factor-beta in chronic rhinosinusitis. Laryngoscope 114:286–290

43. Ichiyama T, Nishikawa M, Yoshitomi T et al (2001) Clarithromycin inhibits NF-kappa B activation in human peripheral blood mononuclear cells and pulmonary epithelial cells. Antimicrob Agents Chemother 45:44–47

44. Kikuchi T, Hagiwara K, Honda Y et al (2002) Clarithromycin suppresses lipopolysaccharide-induced interleukin-8 production by human monocytes through AP-1 and NF-kappa B transcription factors. J Antimicrob Chemother 49:745–755

45. Sharma K, Jin Y, Guo J, Ziyadeh FN (1996) Neutralization of TGF-beta by anti-TGF-beta antibody attenuates kidney hypertrophy and the enhanced extracellular matrix gene expression in STZ-induced diabetic mice. Diabetes 45:522–530